

Effective range analysis of positron-hydrogen collisions

S. J. Ward¹ and J. H. Macek²

¹*Department of Physics, University of North Texas, Denton, Texas 76203*

²*Department of Physics and Astronomy, University of Tennessee, Knoxville, Tennessee 37996
and Oak Ridge National Laboratory, P.O. Box 2009, Oak Ridge, Tennessee 37831*

(Received 10 April 2000; published 13 October 2000)

Humberston [Can. J. Phys. **60**, 591 (1982)], using the Kohn variational method, showed that the range of validity of Wigner's threshold law for positronium formation in positron-hydrogen collisions is extremely narrow for the S wave. To examine the near-threshold behavior, we analyzed *ab initio* calculations using the multichannel effective range theory of Watanabe and Greene [Phys. Rev. A **22**, 158 (1980)] and the single-channel effective range theory of Fabrikant [Opt. Spectrosc. **53**, 131 (1982)] for the positronium-proton channel. We confirmed the presence of a Ramsauer minimum in the $L=0$ elastic cross section for positronium-proton scattering, and found a similar minimum for $L=1$. The near-threshold structure is interpreted in terms of a virtual state, resonances, tunneling through and transmission over a barrier, and quantum suppression.

PACS number(s): 34.85.+x

I. INTRODUCTION

Positronium formation in positron-hydrogen collisions is a fundamental three-body Coulomb process, and is amenable to experimental investigation [1–4]. This process is of interest in astrophysics due to the observation of 511-keV γ rays from solar flares, from the galactic center and from above the galactic center [5–7]. The cross section for antihydrogen formation in antiproton-positronium collisions is related simply to the cross section for positronium formation in positron-hydrogen collisions [8].

The positronium formation cross section in positron-hydrogen collisions in the Ore gap was calculated accurately using a number of different methods. (The Ore gap is the energy region between the onset of positronium formation and the first excitation level of the target atom.) The S -, P -, and D -wave cross sections for positronium formation were computed by Humberston and co-workers using the Kohn and inverse Kohn variational methods [9–14]. Humberston *et al.* [14] showed that the partial cross sections correctly satisfy the Wigner's threshold law [15] but the range of validity is very small for the S wave. Extensive two-center close-coupling calculations were performed [16–21]. Gien [22] employed the Harris-Nesbet method. Archer *et al.* [23] performed a pioneering calculation for the S -wave cross section for positronium formation in positron-hydrogen collisions in the Ore gap. More recently, Igarashi and Toshima [24] and Zhou and Lin [25–27] performed hyperspherical close-coupling calculations for the $L=0, 1, 2, 3, 4, 5$, and 6 partial waves and for the $L=0, 1, 2$, and 3 partial waves, respectively. Very recently, Hu [28] reported K matrices and cross sections for S, P, D , and F waves using modified Faddeev equations. Previously, we employed the hyperspherical hidden crossing method to compute the S -, P -, and D -wave cross sections for positronium formation [29].

The positronium formation cross section was measured for positron collisions with hydrogen [1–3], deuterium [4], alkali metals [30], and noble gases [31]. The measurements of positronium formation for positron collisions from the noble gases were analyzed using Wigner's R -matrix method, which is an effective range theory (ERT) for short-range in-

teractions [31,32]. Humberston *et al.* [14] used this method to fit their variational results close to the positronium formation threshold. While the fit to the variational results for $\sigma_{12}(L=0)$ is good close to threshold, it deviates from the variational results soon after the threshold, with the deviation becoming large near the $n=2$ threshold. Wigner's R -matrix method does not explicitly take into account the polarization potential in either the positron-hydrogen or positronium-proton channels. The polarizability relevant to the initial channel is that of hydrogen, which is fairly small, namely 4.5 a.u.; however, the effective polarizability in the positronium-proton channel is significant, namely, 72 a.u.

Here, we present K matrices and cross sections for the S, P and D waves for positron-hydrogen collisions in the Ore gap that we obtained using the multichannel ERT of Watanabe and Greene [33]. We obtained the ERT parameters by fitting to the *ab initio* calculations of Refs. [14,22]. For simplicity, we also used the single-channel ERT of Fabrikant [34] to analyze the positronium-proton channel. Both ERT's explicitly take into account the polarization potential in the positronium-proton channel. These theories confirm the S -wave Ramsauer minimum in K_{22} found by Van Reeth and Humberston [35], where K_{22} is the element of the K matrix corresponding to positronium-proton scattering. In addition, we found a P -wave Ramsauer minimum in K_{22} . The ERT analysis also provides evidence in the positronium-proton system of an S -wave virtual state and P - and D -wave resonances with negative-energy positions.

The multichannel ERT fits the Kohn variational $\sigma_{12}(L=0)$ well near the positronium formation threshold, and fairly well over the entire Ore gap. The behavior of this cross section is quite striking, with a steep rise near the threshold consistent with Wigner's threshold law, followed by a gently rising plateau. The ERT analysis confirms that Wigner's threshold law [15] is valid only in a very narrow energy range.

We interpret the sharp rise of the S -wave cross section as tunneling through a barrier. The barrier arises from a repulsive centrifugal-type term and an attractive polarization potential. The squared transmission modulus $|T|^2$ fits the steep rise followed by a plateau. We also analyzed the steep rise in

terms of the quantum suppression ratio P [36]. We find that P is quite similar to $|T|^2$; thus positronium formation provides a physical example of quantum suppression. The ERT calculations, the top-of-barrier analysis, and quantum suppression effects illustrate the importance of the polarization potential in the positronium-proton channel.

We outline the ERT's in Sec. II, and give the results in Sec. III. In Sec. IV, we derive for arbitrary L a squared transmission modulus $|T|^2$ for wave propagation through a barrier, and apply it to S -wave positronium formation. In Sec. V, we present the quantum suppression ratio for P , and in Sec. VI we present our conclusions. In the Appendix, we discuss the effect of the polarization potential on the position of the virtual state and resonance poles in the S -matrix. We use atomic units throughout unless explicitly stated.

II. EFFECTIVE RANGE THEORY

The long-range polarization potential $-\mu\alpha/2r^4$ in the positronium-proton channel is important for energies close to threshold. For this potential, an expansion of $k^{2l+1} \cot \delta_l$ in k^2 does not exist, and effective range expressions for short-range interactions do not apply. However, O'Malley *et al.* [37] derived a modified ERT (MERT) applicable to the $-\alpha/2r^4$ polarization potential. They used exact solutions to the Schrödinger equation with the polarization potential [33,38,39]. The solutions are given in terms of Mathieu functions $r^{1/2}M_{\pm\tau}[\ln(k/f)^{1/2}r]$, where $f=\sqrt{\mu\alpha}$ and τ is the order of the Mathieu functions. O'Malley *et al.* [37] expanded the characteristic exponent τ and the ratio $m(\tau) = M_{+\tau}(0)/M_{-\tau}(0)$ about the threshold energy. For $l=0$, the expansion of $k \cot \delta_0$ about $E=0$ contains a number of terms not present in the usual ERT, including a term linear in k and a log term. They found [37]

$$k \cot \delta_0 = -\frac{1}{a_0} + \frac{\pi f^2}{3a_0^2}k + \frac{4f^2}{3a_0}k^2 \ln(0.25fk) + \dots \quad (1)$$

For $l \neq 0$, the leading term in the expansion of $\tan \delta_l$ is proportional to k^2 , and is given by [37]

$$\tan \delta_l = \frac{\pi f^2 k^2}{(2l+3)(2l+1)(2l-1)}. \quad (2)$$

While Eqs. (1) and (2) are appropriate when the potential consists of a short-range part and a polarization potential, the range of applicability in energy is very narrow when the effective polarizability $\mu\alpha$ is large. Furthermore, Eqs. (1) and (2) are for single-channel scattering only. Consequently, Watanabe and Greene [33] and Fabrikant [34] extended the MERT [37] to a broader energy range, and Watanabe and Greene [33] considered a multichannel system. The broader range is achieved by retaining the exact values of the characteristic exponent τ and the ratio m rather than expansions valid only for small f .

A key feature in ERT's is the normalization of the base pair of solutions for the Schrödinger equation with the polarization potential. The base pair is normalized to be energy independent near $r \approx 0$ in order to minimize the energy de-

pendence of a short-range K matrix. The base pair is chosen from a linear combination of $r^{1/2}M_{\pm\tau}[\ln(k/f)^{1/2}r]$ to yield real standing waves for positive energy [33].

Watanabe and Greene [33] applied their quantum defect theory to a multichannel problem: that of the photodetachment of K^- in an energy range where two P channels of K^- , namely, $4s\epsilon p$ and $4p\epsilon s$, are open. The polarization potential in the second channel was explicitly taken into account. The two-channel K matrix was expressed in terms of the quantum defect parameters (η_P, B, \mathcal{G}) that vary rapidly with energy and the parameters (the elements of the matrix K^{P0}) that vary slowly with energy. The quantum defect parameters arise from the polarization potential and depend upon τ and m , whereas the parameters that vary slowly with energy depend upon the short-range interaction.

Watanabe and Greene [33] obtained K^{P0} in the following way. At a single energy, the full physical K matrix K^Z from an *ab initio* calculation was fitted using the elements of K^{P0} as fitting parameters. Since K^{P0} varies slowly with energy, it was taken to be a constant obtained at a single energy where the *ab initio* calculations were most reliable. The fitted K^{P0} was then used over the entire range where only the two channels were open. The effect of the polarization potential in the first channel is taken into account implicitly in the process of fitting the two-channel matrix K^{P0} . We used the same procedure here, except that for $L=0$ we also considered fits where K_{22}^{P0} or $(K_{22}^{P0})^{-1}$ vary linearly with energy.

The full physical K matrix (K^Z) is expressed in terms of the elements of K^{P0} , namely,

$$K^Z = \begin{pmatrix} K_{11}^Z & K_{12}^Z \\ K_{21}^Z & K_{22}^Z \end{pmatrix} = \begin{pmatrix} k_1^{l_1+1/2} & 0 \\ 0 & k_2^{l_2+1/2} \end{pmatrix} \begin{pmatrix} K_{11}^{Z0} & K_{12}^{Z0} \\ K_{21}^{Z0} & K_{22}^{Z0} \end{pmatrix} \begin{pmatrix} k_1^{l_1+1/2} & 0 \\ 0 & k_2^{l_2+1/2} \end{pmatrix}, \quad (3)$$

where

$$K^{Z0} = \begin{pmatrix} K_{11}^{Z0} & K_{12}^{Z0} \\ K_{21}^{Z0} & K_{22}^{Z0} \end{pmatrix} = \frac{1}{Q} \begin{pmatrix} K_{11}^{P0}Q + K_{21}^{P0}K_{12}^{P0}\Gamma_{gf} & K_{12}^{P0} \\ K_{12}^{P0} & K_{22}^{P0}\Gamma_{gg} - \Gamma_{fg} \end{pmatrix}, \quad (4)$$

$Q = \Gamma_{ff} - K_{22}^{P0}\Gamma_{gf}$, and $l_1 = l_2 = L$, and k_1 and k_2 are the wave numbers of the positron and positronium, respectively.

Equations (3) and (4) are inverted to give the fitting parameters K^{P0} ,

$$K^{P0} = \begin{pmatrix} K_{11}^{P0} & K_{12}^{P0} \\ K_{21}^{P0} & K_{22}^{P0} \end{pmatrix} = Q \begin{pmatrix} \frac{K_{11}^{Z0}}{Q} - K_{12}^{Z0}K_{21}^{Z0}\Gamma_{gf} & K_{12}^{Z0} \\ K_{21}^{Z0} & \Gamma_{ff}K_{22}^{Z0} + \Gamma_{fg} \end{pmatrix}, \quad (5)$$

$$K^{P0} = Q \begin{pmatrix} \frac{k_1^{-2l_1-1} K_{11}^Z}{Q} - k_1^{-l_1-1/2} k_2^{-l_2-1/2} (K_{12}^Z)^2 \Gamma_{gf} & k_1^{-l_1-1/2} k_2^{-l_2-1/2} K_{12}^Z \\ k_1^{-l_1-1/2} k_2^{-l_2-1/2} K_{12}^Z & k_2^{-2l_2-1} \Gamma_{ff} K_{22}^Z + \Gamma_{fg} \end{pmatrix}, \quad (6)$$

where

$$Q = \frac{1}{\Gamma_{gg} + \Gamma_{gf} K_{22}^Z} = \frac{1}{\Gamma_{gg} + k_2^{-2l_2-1} \Gamma_{gf} K_{22}^Z}. \quad (7)$$

In these equations, the matrix Γ depends on the quantum defect parameters η_P , B , and \mathcal{G} and is given by

$$\begin{aligned} \Gamma &= \begin{pmatrix} B^{1/2} & 0 \\ B^{-1/2} \mathcal{G} & B^{1/2} \end{pmatrix}^{-1} \begin{pmatrix} \cos \eta_P & \sin \eta_P \\ -\sin \eta_P & \cos \eta_P \end{pmatrix}^{-1} \\ &\times \begin{pmatrix} \cos\left(-\frac{l_2 \pi}{2}\right) & \sin\left(-\frac{l_2 \pi}{2}\right) \\ -\sin\left(-\frac{l_2 \pi}{2}\right) & \cos\left(-\frac{l_2 \pi}{2}\right) \end{pmatrix} \\ &\times \begin{pmatrix} k_2^{l_2+1/2} & 0 \\ 0 & k_2^{-l_2-1/2} \end{pmatrix}, \end{aligned} \quad (8)$$

where

$$\eta_P = \arctan(\eta_1 / \eta_2) - \frac{1}{2} l_2 \pi, \quad (9)$$

$$B = (\eta_1^2 + \eta_2^2)^{-1}, \quad (10)$$

$$\mathcal{G} = -B(\eta_1 \eta_3 + \eta_2 \eta_4), \quad E_2 > 0. \quad (11)$$

The parameters η_1 , η_2 , η_3 , and η_4 depend only upon the characteristic exponent τ and ratio m through

$$\eta_1 = \frac{1}{2} \left[\left(m + \frac{1}{m} \right) + \left(m - \frac{1}{m} \right) \frac{1}{\cos 2\delta} \right], \quad (12)$$

$$\eta_4 = \frac{1}{2} \left[\left(m + \frac{1}{m} \right) - \left(m - \frac{1}{m} \right) \frac{1}{\cos 2\delta} \right], \quad (13)$$

$$\eta_2 = + \frac{1}{2} \left(\frac{1}{m} - m \right) \tan 2\delta, \quad (14)$$

$$\eta_3 = - \frac{1}{2} \left(\frac{1}{m} - m \right) \tan 2\delta, \quad (15)$$

where

$$\delta = \frac{\pi}{2} \left(\tau - l_2 - \frac{1}{2} \right). \quad (16)$$

For positron-hydrogen collisions in the Ore gap, there are two open channels and the effective polarization potential is

significant in the positronium-proton channel. Thus, like Watanabe and Greene [33], we explicitly considered the effective polarization potential in the second channel only, using Eq. (6) and the *ab initio* K matrix at a single energy to obtain the slowly varying matrix K^{P0} . We used this constant value in Eq. (3) to compute K^Z for the entire Ore gap. For $L=0$, we also used the values of the *ab initio* K matrix [14] at two energies to fit K_{22}^{P0} and $(K_{22}^{P0})^{-1}$ to linear functions of k_2^2 .

Fabrikant [34] developed an alternative ERT for the polarization potential. It is for single-channel scattering only, and has the form

$$\tan \delta_l = - \frac{Mc + d}{Ma + b}, \quad (17)$$

where δ_l is the phase shift. The coefficients a, b, c , and d depend only on the polarization potential, i.e., only upon τ and m . Khrebtukov [40] gave explicit analytical expressions for these coefficients, namely,

$$a = \left(\frac{1}{m} - m \right) \cos \pi \tau, \quad (18)$$

$$b = \left(\frac{1}{m} + m \right) \sin \pi \tau + (-1)^l \left(\frac{1}{m} - m \right), \quad (19)$$

$$c = \left(\frac{1}{m} + m \right) \sin \pi \tau - (-1)^l \left(\frac{1}{m} - m \right), \quad (20)$$

$$d = -a. \quad (21)$$

In Eq. (17) M depends on the short-range potential only, is a meromorphic function of energy, and is related to Wigner's R matrix. Furthermore, it has the same analytic properties as Wigner's R matrix, namely, it is an analytic function of energy except for simple poles [34]. The value of M (if applied to the second channel) is identical to $(K_{22}^{P0})^{-1}$ of Watanabe and Greene's ERT [33]. Note also that Eq. (17) is equivalent to Eq. (4.3) of Ref. [37].

For $L=0$ the coupling between the elastic positron-hydrogen channel and the positronium-proton channel is weak, i.e., $K_{12} = K_{21}$ is small and the single-channel ERT of Fabrikant [34] can be used. In this case, $K_{22} \approx \tan \delta_L$. We extracted a value of M at a single energy, and used it for the entire Ore gap. We also used the *ab initio* K_{22} ($\approx \tan \delta_L$) at two energies to fit M and M^{-1} to a linear function of energy.

We used MATHEMATICA to code the ERT's of Watanabe and Greene [33] and Fabrikant [34]. We checked our computed values of τ and m with those tabulated by Khrebtukov [40]. We also checked the quantum defect parameters η_P , B , and \mathcal{G} , with those given by Watanabe and Greene [33] for

TABLE I. Fitted parameters K^{P0} . For $L=0$, K_{11}^{P0} and $K_{12}^{P0} = K_{21}^{P0}$, fitted at $k_1=0.7081$ a.u. For $L=1$, K_{11}^{P0} and $K_{12}^{P0} = K_{21}^{P0}$, fitted at $k_1=0.714$ a.u. For $L=2$, K_{11}^{P0} and $K_{12}^{P0} = K_{21}^{P0}$, fitted at $k_1=0.75$ a.u.

| L | 0 | 1 | 2 |
|-----------------------------|---------------|-------------|----------------------------|
| K_{11}^{P0} | -0.07942^a | 0.79095^a | 0.66064^a 0.71014^b |
| $K_{12}^{P0} = K_{21}^{P0}$ | -0.031971^a | 1.12197^a | 0.40198^a 0.46194^b |
| K_{22}^{P0} | -0.53006^a | 4.44290^a | 0.42800^a 0.54936^b |

^aFitting to the variational results [14,42].

^bFitting to the E8PS results [22].

$L=0$ and with those obtained from the fortran code of Watanabe and Greene [41] for $L=0, 1$, and 2 . In searching for a pole in the single-channel S matrix, we used the fortran code of Khrebtukov [40], which solves $\tan \delta_l = -i$ using $\tan \delta_l$ from Eq. (17).

III. EFFECTIVE-RANGE THEORY RESULTS

A. Results for $L=0$

From the variational calculation of Humberston *et al.* [14] of the K matrix K^Z at $k_1=0.7081$ a.u., we obtained K^{P0} using Eq. (5). We give the elements of K^{P0} in Table I. We used this short-range K matrix in Eqs. (3) and (4) to compute the K matrix and cross sections for the entire Ore gap.

We also used Eq. (5) to compute K_{22}^{P0} at two energies ($k_1=0.7077$ and 0.7083). This enabled us to fit K_{22}^{P0} to two alternative forms, namely, a k_2^2 ,

$$K_{22}^{P0} = \beta + \gamma k_2^2, \quad (22)$$

and

$$(K_{22}^{P0})^{-1} = \beta' + \gamma' k_2^2, \quad (23)$$

where the parameters β , γ , β' , and γ' are -0.53383 , 1.34436 , -1.87319 , and -4.77958 , respectively. We took the elements K_{11}^{P0} and K_{12}^{P0} to have the constant values given in Table I.

Figure 1 compares the three ERT calculations for K_{22} with the variational calculations [14,35]. The three ERT calculations are in which (i) K_{22}^{P0} is taken to be a constant, (ii) K_{22}^{P0} is taken to have the energy dependence of Eq. (22), and (iii) $(K_{22}^{P0})^{-1}$ is taken to have the energy dependence of Eq. (23). All three ERT calculations give excellent agreement with the variational results [14] close to the positronium formation threshold and up to about $k_1^2=0.504$, and reasonable agreement for the entire Ore gap. The ERT calculations in which K_{22}^{P0} has an energy dependence of the form of either Eq. (22) or (23) does better over the entire energy range than the ERT calculation in which K_{22}^{P0} is taken as a constant.

As noted by Van Reeth and Humberston [35], there is a Ramsauer minimum in the positronium-proton elastic cross

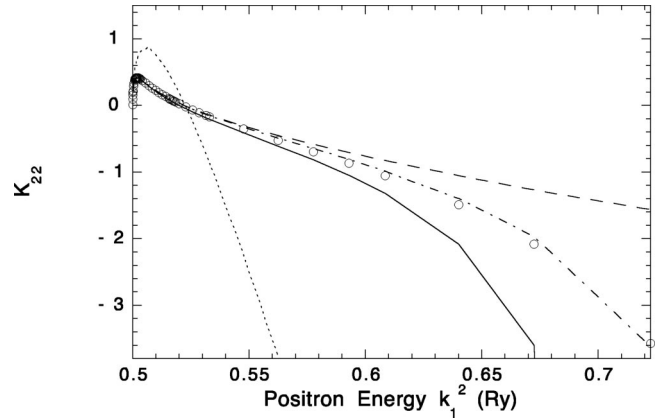


FIG. 1. $L=0$, K_{22} vs the energy of the incident positron k_1^2 (in Ry). The open circles are the variational results [14]. The short-dashed line shows the first two terms of the MERT for $\tan \delta_0$ [37]. The solid, dashed, and the dashed-dot lines are the results obtained using the multichannel ERT [33]. The solid line corresponds to taking K_{22}^{P0} equal to a constant, the dashed line corresponds to using a linear fit for K_{22}^{P0} , and the dashed-dot line corresponds to using a linear fit for $(K_{22}^{P0})^{-1}$.

section as a result of K_{22} passing through zero. The position of the Ramsauer minimum can be estimated from the first two terms of the MERT [37]

$$\tan \delta_0 = k_2 \left(-a_0 - \frac{1}{3} (\pi \mu \alpha k_2) \right), \quad (24)$$

namely,

$$k_2^{RM} = \frac{3|a_0|}{\pi \mu \alpha}. \quad (25)$$

The scattering length $a_0 \equiv \lim_{k \rightarrow 0} \tan \delta_0 / k$ is related to K_{22}^{P0} by $a_0 = f / K_{22}^{P0}$. Using the value of K_{22}^{P0} given in Table I gives the scattering length of -16.0089 a.u. Gien [22], using the enlarged eight state E8S coupled-state calculation [H(1s,2s,2p,3p) and Ps(1s,2s,2p,3p)], obtained a scattering length of -15.89 a.u. Using our value of the scattering length in Eq. (25) gives the Ramsauer minimum at $k_2^{RM} = 0.2123$ a.u., in good agreement with Ref. [14]. It is interesting that, while Eq. (25) gives a good estimate of the position of the Ramsauer minimum, the shape of $\tan \delta_0$ from the MERT agrees poorly with the variational calculation [14] and the two-channel ERT of Watanabe and Greene [33]. Most importantly Eq. (24) predicts a maximum value of $\delta_0 \approx 3|a_0|^2 / 4\pi\mu\alpha \approx \pi/3.7$, whereas the ERT fit gives a value close to $\pi/8$.

The scattering length for the positronium-proton system is large and negative, indicating an $L=0$ virtual state of the positronium-proton system. The behavior of K_{22} near threshold is consistent with the presence of a virtual state; that is, it rises very rapidly after the positronium formation threshold, and reaches a maximum close to threshold, in this case at an energy $E_2 = k_2^2/4 = 8.68 \times 10^{-4}$ a.u. above threshold. At the maximum $K_{22} = 0.41929$, so that the corresponding phase

shift $\delta_0 = \tan^{-1} K_{22} = 0.3969 \approx \pi/8$. The eigenvalue of the K matrix corresponding to positronium-proton scattering, denoted here by \tilde{K}_{22} , has a value very close to K_{22} at maximum, $\tilde{K}_{22} = 0.42005$. Thus, at the maximum, the eigenphase corresponding to positronium-proton scattering is given by $\tilde{\delta}_0 = 0.3988 \approx \pi/8$. Interestingly, for positronium-proton scattering the eigenphase corresponding to positronium-proton scattering for $L=0, 1$, and 2 is approximately $\pi/8(2L+1)$ at the maxima. For short-range interactions and for $L=0$ if there is a virtual state, the phase shift rises rapidly to a value of slightly below $\pi/2$ (or an odd multiple of $\pi/2$). A virtual state corresponds to a pole in the S matrix on the negative imaginary k axis for short-range interactions. For single-channel scattering, a pole in the S matrix corresponds to $\tan \delta_l = -i$. We obtained an estimate of the position of the virtual state pole by approximating the two-channel problem as a single-channel problem, that of positronium-proton scattering, and locating the pole in the single-channel S matrix. This approximation should be good for $L=0$ where the coupling between the two channels is weak. Using just the first term of the MERT [37], Eq. (1) gives the position on the pole to be at $k_p = -i/|a_0| = -0.0624i$, which is on the negative imaginary k axis. However, if one uses the first two terms of the MERT [37], Eq. (1), the pole is at $k_p = -0.0169 - 0.05749i$, which is slightly off the negative imaginary k axis. If one uses the ERT of Fabrikant [34] with the exact expressions for τ and m , and takes $M = (K_{22}^{P0})^{-1}$ to be a constant, the pole is slightly closer to the real axis at $k_p = -0.00096 - 0.037i$. The position of the pole changes only slightly if M or $(M)^{-1}$ is fitted to a form linear in energy. This is the first prediction of a virtual state of the positronium-proton system. Because it does not occur at the usual position on the imaginary k axis, and because this anomaly is related to the polarization potential, we give a more complete discussion of virtual states in the Appendix.

Figure 2 compares the three ERT calculations for K_{12} with the variational calculations [14]. The ERT calculation in which K_{22}^{P0} is taken to be a constant gives excellent agreement with the variational calculations close to the positronium formation threshold, and reasonable agreement for the entire Ore gap. However, the ERT calculations in which K_{22}^{P0} has the energy dependence of Eq. (22) or (23) gives better agreement with the variational results for the entire Ore gap. In all cases, K_{12} satisfies Wigner's threshold law [15], namely, it is proportional to $k_2^{L+1/2}$ near threshold.

Humberston *et al.*'s variational results satisfy Wigner's threshold law [15]

$$\sigma_{12} \propto k_2^{2L+1}, \quad (26)$$

but only over a very small energy range for the S wave [14]. The cross section displays an infinite slope at threshold, maximizes at an energy 1.48×10^{-3} a.u. above threshold, and changes abruptly to a gently rising plateau over the remainder of the Ore gap. There is a small peak at the transition between the steep rise and the plateau.

This behavior was analyzed in Ref. [14] using Wigner's R matrix (ERT) [32] with a five-parameter fit for each partial

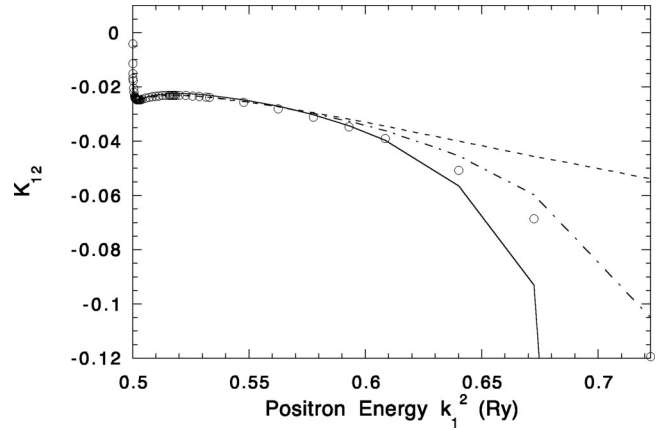


FIG. 2. $L=0$, K_{12} vs the energy of the incident positron (in Ry). The open circles are the variational results [14]. The solid, dashed, and the dashed-dot lines are the multichannel ERT results. K_{11}^{P0} and K_{12}^{P0} are taken as constants. The solid line corresponds to taking K_{22}^{P0} to be a constant, the dashed line corresponds to using a linear fit for K_{22}^{P0} , and the dashed-dot line corresponds to using a linear fit for $(K_{22}^{P0})^{-1}$.

wave. The fit to Wigner's R matrix gives the correct threshold behavior and a steep rise of $\sigma_{12}(L=0)$ near threshold, but, after the maximum in the cross section, it begins to deviate from the variational result. The deviation becomes quite significant at the $n=2$ threshold, owing to the rapid decrease of the R matrix results with energy. Figure 3 compares the three ERT calculations with the variational results [14]. All three ERT calculations obtain a steep rise and a small peak near threshold. The cross section computed with a constant K_{22}^{P0} decreases with energy but not as significantly as the Wigner's R matrix calculation. The ERT calculations in which K_{22}^{P0} is taken to have the energy dependence of either Eq. (22) or (23) agree well with the variational results [14] up to a position energy k_1^2 of about 0.65 a.u. These ERT calculations illustrate the importance of explicitly taking into account the polarization potential in the positronium-proton channel.

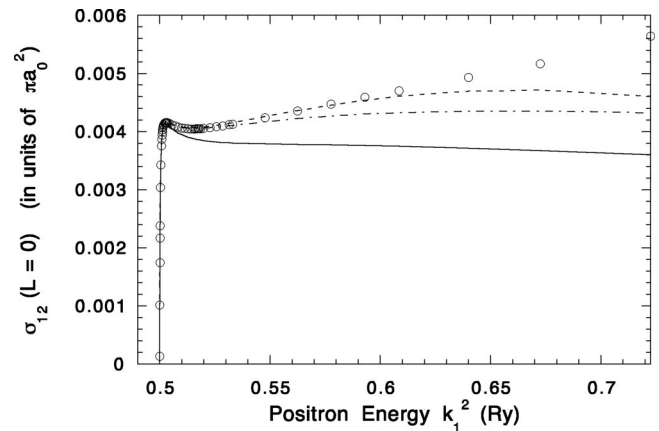


FIG. 3. $L=0$ partial contribution to the cross section (in units of πa_0^2) for positronium formation vs the energy of the incident positron (in Ry). See the caption of Fig. 2.

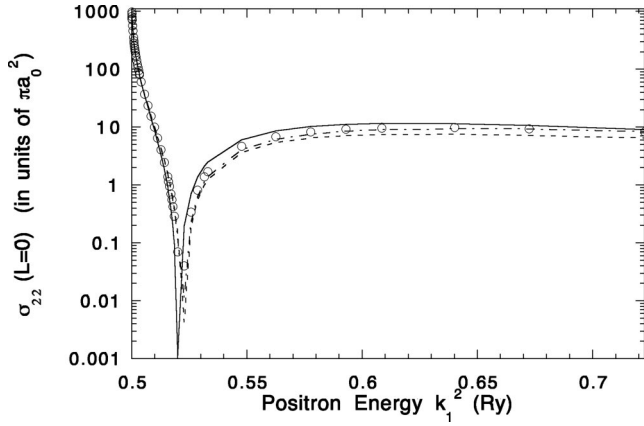


FIG. 4. $L=0$ partial contribution to the cross section (in units of πa_0^2) for elastic positronium-proton scattering vs the energy of the incident positron (in Ry). See the caption of Fig. 2.

Figure 4 compares the ERT σ_{22} with the variational results [14]. The cross section rises rapidly as the energy decreases toward the positronium formation threshold. The zero-energy cross section is large ($1025\pi a_0^2$) due to a large scattering length. The Ramsauer minimum is clearly evident in the cross section at a positron energy of approximately 0.52 Ry. All three ERT calculations give a virtual state, a Ramsauer minimum, and a good fit to the variational results over the entire energy range of the Ore gap. The ERT calculations in which K_{22}^{P0} is given an energy dependence of either Eq. (22) or (23) does better in reproducing the position of the Ramsauer minimum than the ERT calculations in which K_{22}^{P0} is taken to be a constant. The ERT calculation in which K_{22}^{P0} has the form of Eq. (23) does better in fitting to the variational results over the whole Ore gap than the other ERT calculations.

Our focus in this paper is on positronium formation and elastic positronium-proton scattering in the Ore gap. We

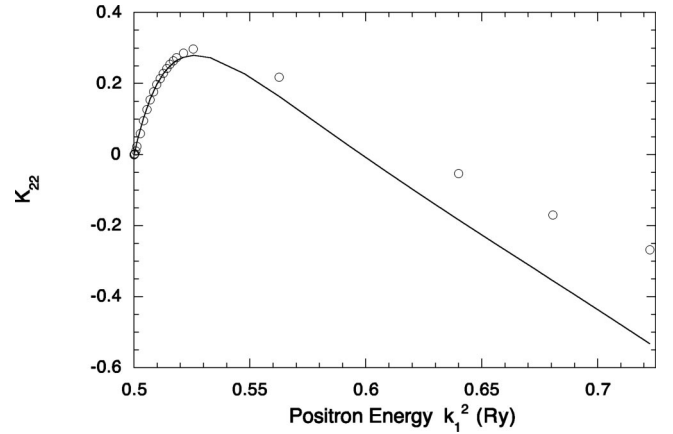


FIG. 5. $L=1$, K_{22} vs the energy of the incident positron (in Ry). The open circles are the variational results [14]. The solid line is multichannel ERT results.

note, however, that we did not obtain good agreement between the multichannel ERT calculations of K_{11} and σ_{11} for all partial waves.

B. Results for $L=1$

We computed the short-range K matrix K^{P0} using Eq. (5) and the variational K matrix (K^Z) of Humberston *et al.* [14] at $k_1=0.714$ a.u. At $k_1=0.714$ a.u. the magnitude of the ratio of K_{22} to K_{12} from the variational calculation is the largest. In Table I we give the fitted elements of K^{P0} which we used for the entire Ore gap. In Table II we give the $L=1$ quantum defect parameters η_p , B , and \mathcal{G} . Note, that B and \mathcal{G} are very large and positive for small kf , but decrease rapidly with increasing energy. As stated by Watanabe and Greene [33], the rapid variation of the amplitudes of B and \mathcal{G} in the region of small kf arises from the penetration of the effective centrifugal barrier $(L+1/2)^2/r^2$. At large kf , B approaches unity and \mathcal{G} vanishes.

Figure 5 compares the ERT fit of K_{22} with the variational

TABLE II. Values of quantum-defect parameters for $L=1$. Positive energies $0.05 \leq kf \leq 5$. Numbers in brackets denote powers of 10.

| kf | k_2 | B | η | η/π | \mathcal{G} |
|-------|-----------|----------|-----------|------------|---------------|
| 5[-2] | 5.893[-3] | 5.075[1] | -1.597[0] | -5.083[-1] | 1.909[3] |
| 1[-1] | 1.179[-2] | 2.548[1] | -1.622[0] | -5.164[-1] | 4.765[2] |
| 2[-1] | 2.357[-2] | 1.288[1] | -1.671[0] | -5.318[-1] | 1.184[2] |
| 3[-1] | 3.536[-2] | 8.699[0] | -1.717[0] | -5.466[-1] | 5.217[1] |
| 4[-1] | 4.714[-2] | 6.622[0] | -1.762[0] | -5.609[-1] | 2.901[1] |
| 5[-1] | 5.893[-2] | 5.382[0] | -1.806[0] | -5.748[-1] | 1.830[1] |
| 6[-1] | 7.071[-2] | 4.560[0] | -1.848[0] | -5.883[-1] | 1.251[1] |
| 7[-1] | 8.250[-2] | 3.976[0] | -1.890[0] | -6.014[-1] | 9.020[0] |
| 8[-1] | 9.428[-2] | 3.540[0] | -1.930[0] | -6.143[-1] | 6.767[0] |
| 9[-1] | 1.061[-1] | 3.203[0] | -1.970[0] | -6.269[-1] | 5.229[0] |
| 1[0] | 1.179[-1] | 2.934[0] | -2.008[0] | -6.393[-1] | 4.134[0] |
| 2[0] | 2.357[-1] | 1.753[0] | -2.367[0] | -7.535[-1] | 7.367[-1] |
| 3[0] | 3.536[-1] | 1.385[0] | -2.690[0] | -8.563[-1] | 1.865[-1] |
| 4[0] | 4.714[-1] | 1.216[0] | -2.990[0] | -9.518[-1] | 3.300[-2] |
| 5[0] | 5.893[-1] | 1.126[0] | -3.273[0] | -1.042[0] | -1.660[-2] |

results [14]. The figure shows good agreement near the positronium formation threshold, and reasonable agreement for the entire Ore gap. Actually, very close to the threshold there is a significant disagreement between the ERT and variational results which is not apparent in the figure due to the smallness of K_{22} in this region. Very close to threshold, the ERT results are in accord with O'Malley *et al.*'s Eq. (2), but the variational results are not. Just above threshold, $k_1 = 0.70712$ a.u. ($k_2^2/2\mu = 9.35 \times 10^{-6}$ a.u.), the variational results are lower than the ERT results by a factor of 12. However, by $k_1 = 0.71$ a.u. ($k_2^2/2\mu = 2.05 \times 10^{-3}$ a.u.), the variational and ERT results agree by about 7%. The matrix element K_{22} rises rapidly from the positronium formation threshold to a maximum, after which it decreases more slowly than the initial rise, passes through zero (the Ramsauer minimum), and then continues to decrease. The behavior of $L=1$ is remarkably similar to that of $L=0$ although for $L=1$ the rapid rise near the threshold is not as sharp for $L=0$ and the Ramsauer minimum occurs at a higher energy.

The similarity of K_{22} for the two partial waves, $L=0$ and 1, is at first surprising, because there is a repulsive angular momentum barrier for $L=1$, but not for $L=0$. We argue in Sec. IV that this similarity is expected on the basis of Mathieu's equation, where there is an effective inverted oscillator "potential," as well as a constant-energy-like term, $-(L+1/2)^2$, for all partial waves. The combination of these two terms means that there are barrier penetration effects present even for $L=0$. These effects were discussed in Ref. [45] using a top-of-barrier theory employing parabolic cylinder functions, and are further discussed in Sec. IV.

The ERT calculation gives the maximum in K_{22} at $k_1 = 0.725$ a.u. and the Ramsauer minimum at k_1 between 0.77 and 0.78 a.u. At the maximum $K_{22} = 0.2798$. The maximum in the eigenvalue of the K matrix \tilde{K}_{22} , corresponding to the positronium-proton channel, occurs at $k_1 = 0.717$ a.u. The eigenphase $\tilde{\delta}_{22}(\tilde{\delta}_{22} = \tan^{-1} \tilde{K}_{22})$ at the maximum of \tilde{K}_{22} is 0.134 which is approximately $\pi/24 = \pi/8(2L+1)$ for $L=1$.

The sharp rise of K_{22} close to the positronium formation threshold indicates an $L=1$ resonance in the positronium-proton channel. We searched for a pole in the single-channel S matrix corresponding to the elastic positronium-proton scattering, although we recognize that the coupling between the two channels is not generally negligible for $L=1$. Near threshold all elements of the K matrix vanish, and the single-channel ERT of Fabrikant [34] with a constant M gives a first estimate of the pole location. We found a pole at $k_2 = 0.095 - 0.168i$, or equivalently at an energy $E_2 = k_2^2/4 = E_r - i(\Gamma/2) = -0.0048 - (i/2)0.016$. The pole is at a negative energy E_r , and the width Γ is positive and relatively large, of the order of 0.1 times the width of the entire Ore gap. We interpret this pole as a resonance with a negative-energy position. Since we used the single-channel approximation, this calculation only suggests the possibility of a resonance.

Figures 6 and 7 compare the ERT and variational results [14] of K_{12} and σ_{12} , respectively. The agreement between the ERT and variational results is excellent close to the positronium formation threshold, and very good over the entire

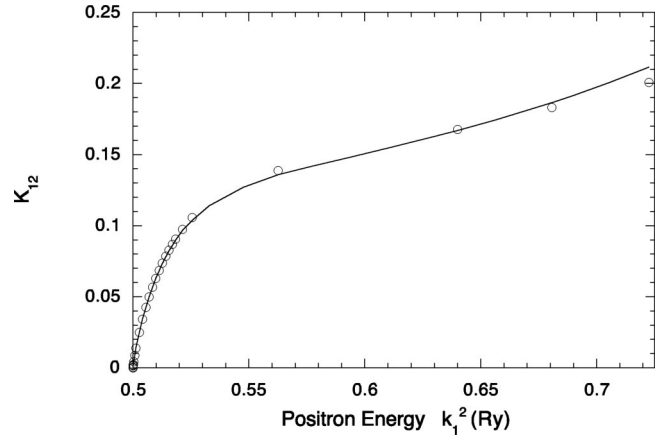


FIG. 6. $L=1$, K_{12} vs the energy of the incident positron (in Ry). See the caption of Fig. 5.

Ore gap. The ERT confirms that the variational results [14] satisfy Wigner's threshold law [15].

Figure 8 compares the ERT fit of σ_{22} with the variational results [14]. It shows that the ERT fit and variational results agree well near the positronium formation threshold, and reasonably well for the entire Ore gap. There is a disagreement between the ERT and variational results very close to threshold due to the disagreement in K_{22} between the two sets of results. However, by $k_1 = 0.71$ a.u., the ERT and variational results agree to within 13%. The cross section σ_{22} rises rapidly from threshold to a peak value of $23\pi a_0^2$ at $k_1 = 0.716$ a.u., decreases to zero at the Ramsauer minimum, and then increases slowly with energy up to the $n=2$ threshold of hydrogen. This behavior is well reproduced by the ERT, indicating that the structure has its origin in the strong polarization potential in this particular channel.

C. Results for $L=2$

In Table III we give the $L=2$ quantum defect parameters η_p , B , and \mathcal{G} . We fitted the short-range K matrix K^{P0} using data from the inverse Kohn variational calculation of the K matrix [14,42] at $k_1 = 0.75$ a.u. In Table I we give the

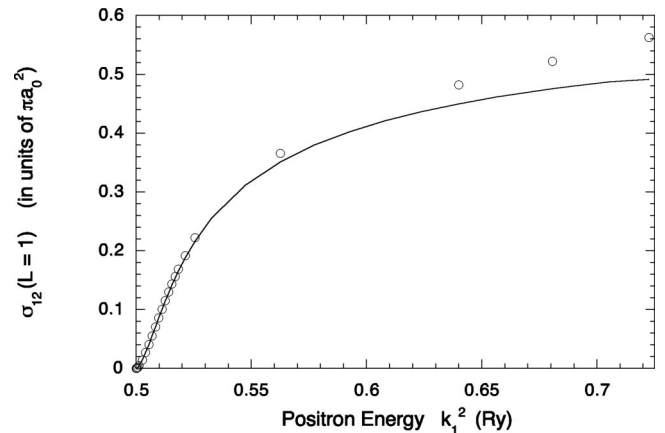


FIG. 7. $L=1$ partial contribution to the cross section (in units of πa_0^2) for positronium formation vs the energy of the incident positron (in Ry). See the caption of Fig. 5.

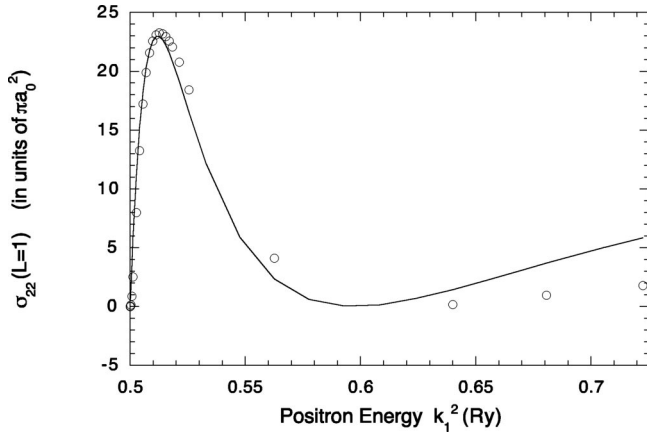


FIG. 8. $L=1$ partial contribution to the cross section (in units of πa_0^2) for elastic positronium-proton scattering vs the energy of the incident positron (in Ry). See the caption of Fig. 5.

fitted elements of K^{P0} . We used the inverse Kohn rather than the Kohn results, since we are informed [42] that the former are more reliable.

We also fitted the short-range matrix K^{P0} using the algebraic enlarged eight pseudostate Harris-Nesbet E8PS calculation of Gien [22] at $k_1=0.75$ a.u. We give these fits in Table I. The wave function in the E8PS scheme is comprised of the (pseudo-)states $H(1s, 2\bar{s}, 2\bar{p}, 3\bar{d})$ and $Ps(2s, 2\bar{s}, 2\bar{p}, 3\bar{d})$ together with a large number of correlation terms. The dipole polarizability of $H(1s)$ and $Ps(1s)$ [43] were taken into account by the $H(2\bar{p})$ and $Ps(2\bar{p})$ pseudostates, respectively [44]. The $H(3\bar{d})$ and $Ps(3\bar{d})$ pseudostates were used to take into account the quadrupole effects.

The inverse Kohn results of K_{22} are not in accord with the MERT of O'Malley *et al.*'s [37] Eq. (2), whereas the E8PS

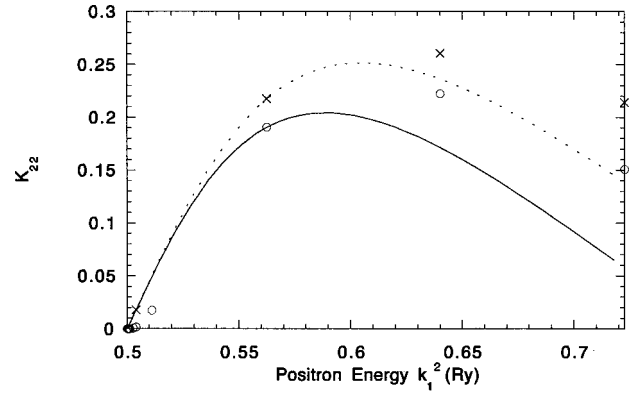


FIG. 9. $L=2$, K_{22} vs the energy of the incident positron (in Ry). The open circles are the inverse Kohn variational results [14,42]. The solid line is the multichannel ERT fit to the inverse Kohn K matrix at $k_1=0.75$ a.u. The crosses are the E8PS results [22]. The dashed line is the multichannel ERT fit to the E8PS K matrix at $k_1=0.75$ a.u.

results of K_{22} are. At $k_1=0.71$ a.u., K_{22} of the inverse Kohn calculation is about a factor of 10 smaller than K_{22} of the E8PS calculation. Humberston *et al.* [14] stated that their $L=2$ results are less well converged than their $L=0$ and 1 results, and that their $L=2$ results are probably less accurate than those of Gien [22]. For $L=0$ and 1 there is much better agreement between the inverse Kohn and E8PS results than there is for $L=2$. This is in accord with our findings. For instance, at $k_1=0.71$ a.u. the two *ab initio* calculations of K_{22} agree within 3% for $L=0$ and 1, but disagree strongly for $L=2$.

Figure 9 shows K_{22} vs the positron energy. This figure compares the ERT fit to the inverse Kohn and E8PS results, as well as the *ab initio* inverse Kohn and E8PS calculations. The two ERT calculations agree well near threshold and both

TABLE III. Values of quantum-defect parameters for $L=2$. Positive energies $0.05 \leq kf \leq 6$. Numbers in brackets denote powers of 10.

| kf | k_2 | B | η | η/π | \mathcal{G} |
|----------|-----------|-----------|-----------|------------|---------------|
| 5[-2] | 5.893[-2] | 2.759[-2] | -3.142[0] | 1.000[0] | 1.337(4) |
| 1[-1] | 1.179[-2] | 5.519[-2] | -3.141[0] | -9.999[-1] | 3.340[3] |
| 2[-1] | 2.357[-2] | 1.104[-1] | -3.141[0] | -9.997[-1] | 8.335[2] |
| 3[-1] | 3.536[-2] | 1.655[-1] | -3.139[0] | -9.993[-1] | 3.694[2] |
| 4[-1] | 4.714[-2] | 2.204[-1] | -3.138[0] | -9.988[-1] | 2.069[2] |
| 5[-1] | 5.893[-2] | 2.747[-1] | -3.136[0] | -9.983[-1] | 1.317[2] |
| 6[-1] | 7.071[-2] | 3.283[-1] | -3.134[0] | -9.977[-1] | 9.086[1] |
| 7[-1] | 8.250[-2] | 3.810[-1] | -3.132[0] | -9.970[-1] | 6.625[1] |
| 8[-1] | 9.428[-2] | 4.324[-1] | -3.130[0] | -9.964[-1] | 5.028[1] |
| 9[-1] | 1.061[-1] | 4.825[-1] | -3.128[0] | -9.958[-1] | 3.934[1] |
| 1[0] | 1.179[-1] | 5.311[-1] | -3.127[0] | -9.995[-1] | 3.152[1] |
| 2[0] | 2.357[-1] | 9.055[-1] | -3.128[0] | -9.956[-1] | 6.767[0] |
| 3[0] | 3.536[-1] | 1.083[0] | -3.175[0] | -1.011[0] | 2.462[0] |
| 4[0] | 4.714[-1] | 1.139[0] | -3.266[0] | -1.040[0] | 1.112[0] |
| 5[0] | 5.893[-1] | 1.142[0] | -3.388[0] | -1.078[0] | 5.664[-1] |
| 5.660[0] | 6.671[-1] | 1.132[0] | -3.479[0] | -1.108[0] | 0.375[-1] |
| 6[0] | 7.071[-1] | 1.125[0] | -3.529[0] | -1.123[0] | 3.066[-1] |

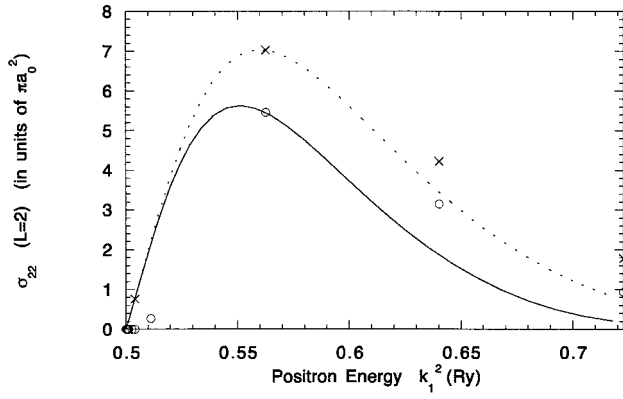


FIG. 10. $L=2$ partial contribution to the cross section (in units of πa_0^2) for elastic positronium-proton scattering vs the energy of the incident positron (in Ry). See the caption of Fig. 9.

satisfy the MERT of O'Malley *et al.* [37]. The E8PS calculation and the corresponding ERT fit agree well at $k_1 = 0.71$ a.u., and agree reasonably well over the entire Ore gap. In contrast, the inverse Kohn results of K_{22} are too low near threshold. We suspect that the polarizability of Ps(1s) is inadequately described in the inverse Kohn results near threshold. This effect is remedied by using the inverse Kohn results at an energy away from threshold then extrapolating to threshold using the multichannel ERT.

The behavior of K_{22} for $L=2$ is similar to the behavior of K_{22} for $L=0$ and 1. It rises from the threshold, reaches a maximum and then decreases with increasing energy up to the $n=2$ threshold. The ERT fit of K_{22} to the E8PS calculation has a maximum value of 0.2417 at $k_1 = 0.7783$ a.u. The maximum occurs at a higher energy for $L=2$ than for $L=0$ and 1, and the rise from threshold is not as rapid. This is in accord with Eq. (2).

We found a pole in the single-channel S matrix corresponding to elastic positronium-proton scattering at $k_2 = 0.2569 - 0.3139i$ which corresponds to an energy of $E_2 = -0.008 - 0.04i$. Thus, as for $L=1$, the pole is at a negative energy and the width is large (relative to the Ore gap) and positive. It corresponds to a resonance with a negative energy position.

Even though K_{22} decreases with energy after its maximum, it does not vanish in the Ore gap, and thus, unlike $L=0$ and 1, there is no Ramsauer minimum for $L=2$. However, the diagonalized matrix element \tilde{K}_{22} does go through zero before the $n=2$ threshold. Thus the second eigenchannel shows a Ramsauer minimum, even though the physical second channel does not. The value of the eigenphase corresponding to elastic positronium-proton scattering is approximately $\pi/40$ at the maximum.

Figures 10, 11, and 12 show σ_{22} , K_{12} , and σ_{12} , respectively, vs the positron energy computed using the ERT fitted to the inverse Kohn calculation, and the E8PS together with the *ab initio* inverse Kohn and E8PS calculations. The fitted E8PS and the *ab initio* E8PS calculations agree well near threshold, and reasonably well for the entire Ore gap. The peak value of σ_{22} from the ERT fit to the E8PS calculation is $7\pi a_0^2$, and occurs at $k_1 = 0.747$ a.u.

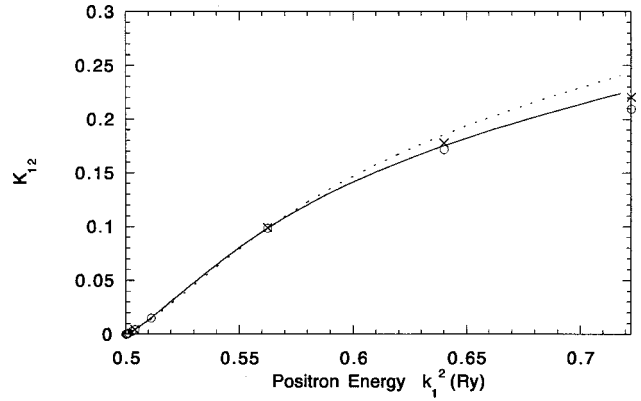


FIG. 11. $L=2$, K_{12} vs the energy of the incident positron (in Ry). See the caption of Fig. 9.

IV. TOP-OF-BARRIER ANALYSIS

The ERT fits to *ab initio* calculations show that the considerable structure in the positronium-proton channel relates closely to the large effective polarization potential in that channel. It should, therefore, be possible to interpret the structure solely in terms of positronium motion in a polarization potential. In this section we show that Wigner's threshold law relates to tunneling through a barrier. The barrier is due to the combined effect of a repulsive centrifugal-type term $(L+1/2)^2/2\mu\rho^2$ and an attractive polarization potential $-\alpha/2\rho^4$, where ρ is the Jacobi coordinate of the center of mass of positronium with respect to the proton. Qualitatively, such tunneling ceases at an energy $k_2^2/2\mu$ greater than the height of the barrier, thus this would suggest that σ_{12} rises with energy as $k_2^{(L+1/2)}$ up to an energy of the order of the top of the barrier, after which it would vary much more slowly. This aspect of the dynamics is included in the ERT via the Mathieu functions and is seen in the ERT fits reported in Sec. III. In this section we relate this behavior to top-of-barrier motion using a formula we employed in connection with our $L=1$ hyperspherical hidden crossing calculations of Ref. [29].

Tunneling through a barrier can be treated via the WKB

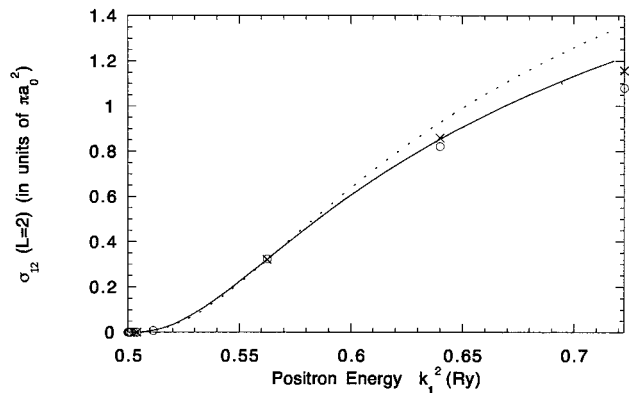


FIG. 12. $L=2$ partial contribution to the cross section (in units of πa_0^2) for positronium formation vs the energy of the incident positron (in Ry). See the caption of Fig. 9.

approximation; however, that theory can only be used for energies well below the top of the barrier. It is necessary to go beyond the WKB approximation to interpret the threshold region. Two theories have been given which do this. One is the top-of-barrier theory of Refs. [29] and [45], which places tunneling and motion above the barrier on an equal footing, and is described in this section. The other is the ‘‘quantum suppression’’ analysis of Ref. [36] discussed in Sec. V.

The cross section that takes into account tunneling through, and motion above, the barrier (Ref. [29]) is given by

$$\sigma_{12}^{(L)} = |T|^2 \sigma_{12}^{(L)}(HC) \quad (27)$$

where $\sigma_{12}^{(L)}(HC)$ is the unmodified hidden crossing cross section, and $\sigma_{12}^{(L)}$ is the hidden crossing cross section that takes into account motion below and above the barrier. In Eq. (27), $|T|^2$ is the transmission modulus squared, and is given by

$$|T|^2 = \frac{1}{1 + \exp(2\pi a)}, \quad (28)$$

where for $E = (k_2^2/2\mu) - 0.25 < V(R_{TOB})$,

$$a = \frac{1}{\pi} \int_{R_1}^{R_2} \sqrt{2(V(R) - E)} dR, \quad (29)$$

and for $E > V(R_{TOB})$,

$$a = \frac{-i}{\pi} \int_{R_1}^{R_2} \sqrt{2(E - V(R))} dR. \quad (30)$$

In Eqs. (29) and (30), R is the hyper-radius, and R_{TOB} is the top-of-barrier position. In Eq. (29), R_1 and R_2 are the zeros of $q(R) = \sqrt{2(V(R) - E)}$, whereas in Eq. (30) $R_1 = R_2^*$ are the complex roots of $q(R) = \sqrt{2(V(R) - E)}$. In Ref. [29], we considered two potentials $V(R)$, namely, $V(R) = \varepsilon_2(R) - \frac{1}{2}(1/4R^2) = \varepsilon_2'(R)$, in accordance with the hidden crossing theory [Eq. (10) of Ref. [29] or Eq. (4.14) of Ref. [47]] and $V(R) = \varepsilon_2(R) - \frac{1}{2}\langle \varphi_2 | (d^2 \varphi_2 / dR^2) \rangle$ in accordance with the one-Sturmian correction to the hidden crossing theory [Eq. (17) of Ref. [29]]. The asymptotic form of $V(R) = \varepsilon_2'(R)$ is given by Eq. (105) of Ref. [48]. The asymptotic form of the potential $V(R) = \varepsilon_2(R) - \frac{1}{2}\langle \varphi_2 | (d^2 \varphi_2 / dR^2) \rangle$ is given by Eqs. (107) and (109) of Ref. [48]. It contains a repulsive centrifugal term $L(L+1)/2\mu\rho^2$ and an attractive polarization potential $-\alpha/2\rho^4$ as well as a small repulsive $1/\rho^4$ potential that is unique to the hyperspherical theory. In Ref. [29] a barrier was noted in both potentials for $L=1$.

A strict application of the hidden crossing theory would also have a factor $|T_{\text{WKB}}|^2$, but that factor would only include tunneling, i.e.,

$$|T_{\text{WKB}}|^2 = \exp[-2\pi a], \quad E < V(R_{TOB}), \quad (31)$$

$$|T_{\text{WKB}}|^2 = 1, \quad E > V(R_{TOB}),$$

where R_{TOB} is the top-of-barrier position. It was recognized in Ref. [29] that the WKB factor is not reliable when two

turning points (R_1 and R_2) are close together, thus the expression in Eq. (28) was used.

In Ref. [29] we considered $|T|^2$ for $L=1$. Here we demonstrate that a barrier is present even for $L=0$, where there is no centrifugal barrier. Because of the significant effective polarization potential in the positronium-proton channel one should use Mathieu functions to propagate the wave in the positronium-proton channel to large distance. Vogt and Wannier [38] showed that the solutions to the Schrödinger equation, corresponding to the polarization potential $-\alpha/2r^4$, are given by $r^{1/2}M_{\pm\tau}[\ln(k/f)^{1/2}r]$. They satisfied the equation

$$\left[x^2 \frac{d^2}{dx^2} + x \frac{d}{dx} - \left(L + \frac{1}{2} \right)^2 + kf(x^2 + x^{-2}) \right] M_{\pm\tau}[\ln x] = 0, \quad (32)$$

where the radial variable r is related to the scaled variable x by $x = (k/f)^{1/2}r$. A further change of variable $x = e^\varphi$ reduces this equation to the standard form of the Mathieu equation

$$\left(\frac{d^2}{d\varphi^2} - \left(L + \frac{1}{2} \right)^2 + 2kf \cosh(2\varphi) \right) M_{\pm\tau}(\varphi) = 0. \quad (33)$$

The change of variable $x = (k/f)^{1/2}r$ [39] introduced the Langer factor $(L+1/2)^2 - L(L+1) = 1/4$. Thus there is a repulsive centrifugal-type term $(L+1/2)^2/r^2$ present even for $L=0$. The repulsive term and the attractive polarization potential result in a barrier even for $L=0$. The transmission modulus squared $|T|^2$ for tunneling through the barrier is given by Eq. (28), where the parameter a is written as

$$a = \frac{1}{\pi} \int_{\rho_1}^{\rho_2} \sqrt{2\mu(V(\rho) - E_2)} d\rho, \quad (34)$$

using Jacobi coordinates. In Eq. (34), ρ_1 and ρ_2 are the real roots of $\sqrt{2\mu(V(\rho) - E_2)}$. Equation (34) is the appropriate form for the parameter a for $V(\rho) > E_2 = k_2^2/2\mu$. The form appropriate for $V(\rho) < E_2$ is analogous to Eq. (30). The asymptotic form of $V(\rho)$ contains just two terms, the repulsive term and the attractive polarization potential:

$$V(\rho) = \frac{(L+1/2)^2}{2\mu\rho^2} - \frac{\alpha}{2\rho^4}. \quad (35)$$

With the asymptotic potential, the integral for a can be evaluated analytically. One obtains

$$a = \frac{L+1/2}{2} \frac{1-b}{\sqrt{1+b}} {}_2F_1 \left[\frac{1}{2}, \frac{3}{2}; 2; \frac{1-b}{1+b} \right], \quad (36)$$

where

$$b = \frac{2\sqrt{\mu\alpha}k_2}{(L+1/2)^2}. \quad (37)$$

Expanding Eq. (36) about the threshold energy for positronium formation gives

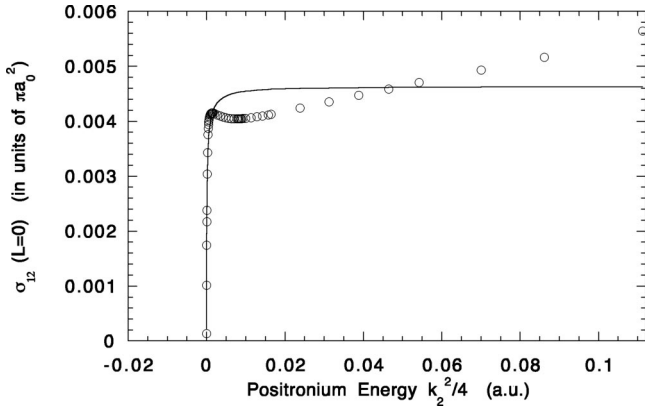


FIG. 13. Comparison of the TOB factor $|T|^2$ with the variational results [14] for the S -wave cross section for positronium formation $\sigma_{12}(L=0)$. The TOB factor $|T|^2$ for the figure is normalized at the peak in the variational results ($k_2=0.077\,018$ a.u., $k_2^2/4=1.482 \times 10^{-3}$ a.u.). The open circles are the variational results. The solid line is the factor $|T|^2$.

$$|T|^2 \approx e^{-2\pi a} \approx \left(\frac{2\sqrt{\mu\alpha}k_2}{8(L+1/2)^2} \right)^{2L+1}. \quad (38)$$

Hence the cross section for positronium formation using Eqs. (27), (28), and (36) correctly satisfies Wigner's threshold law. We see the importance of the repulsive centrifugal-type term $(L+1/2)^2/2\mu\rho^2$ to obtain Wigner's threshold law. At the top of the barrier, $b=1$, $a=0$, and $|T|^2=1/2$. Using the asymptotic form of the potential [Eq. (35)] the position of the top of the barrier is estimated to be at $\rho_{TOB} = \sqrt{2\mu\alpha/(L+1/2)^2}$ and the height to be $V_{max}=k_{TOB}^2/2\mu = (L+1/2)^4/8\mu^2\alpha$. For $L=0$, the position of the top of the barrier is estimated to be $\rho=24$ a.u., or in terms of the hyper-radius to be at $R=34$ a.u. The height of the $L=0$ barrier is extremely small, namely, $0.000\,054$ a.u. This small value accounts for the sudden change of the positronium formation cross section near threshold. Even for $L=1$, the energy corresponding to the height of the barrier, 4.4×10^{-3} a.u., is considerably smaller than the region of applicability of the ERT.

Figure 13 compares $|T|^2$ with the variational [14] S -wave positronium formation cross section. For the purpose of the figure, we normalized $|T|^2$ at the peak of the variational results of $\sigma_{12}(k_2=0.077\,01$ a.u.). It can be seen that $|T|^2$ has the correct general behavior, namely, a very steep rise near threshold followed by a more gently rising plateau. At the cross-section peak, the positronium kinetic energy $k_2^2/2\mu$ is about five times the height of the potential of the top of the barrier, i.e., well above the top of the barrier. Although $|T|^2$ is similar to the shape of the positronium formation cross section, it fails to reproduce the small peak in the variational results [14] and in the ERT fits (see Fig. 3). This small peak is probably due to the reflection from the barrier back into the interaction region omitted in the top-of-barrier theory. Aside from this effect, the top-of-barrier theory accurately represents the structure seen in the more complete ERT.

V. QUANTUM SUPPRESSION

In Sec. IV we saw that the WKB approximation to the Mathieu functions accounts only for Wigner's threshold law, but fails at an energy as small as 5.4×10^{-5} a.u. above the threshold. The reduction of excitation cross sections below the expected WKB value has been called "quantum suppression," and has been analyzed for a model system by Cote *et al.* [36]. To determine whether the near-threshold S -wave cross section for positronium formation is a physical example of quantum suppression, we applied the analysis of Ref. [36], where the suppression is related to a factor P , the ratio of the quantum-mechanical probability (K_{qm}) for entering the well to the semiclassical probability (K_{sc}), i.e.,

$$P = \frac{K_{qm}}{K_{sc}}, \quad (39)$$

where

$$K_{qm} = \frac{|u^{in}(\rho_{in}^*)|^2}{|u^{out}(\rho_{out}^*)|^2} = |u^{in}(\rho_{in}^*)|^2 \sin^2 \delta_0, \quad (40)$$

and δ_0 is the S -wave phase shift. The function $u(\rho)$ is the S -wave solution to the Schrödinger equation, normalized according to

$$u^{out}(\rho) \sim \frac{\sin(k_2\rho + \delta_0)}{\sin \delta_0}. \quad (41)$$

The radius ρ_{in}^* is where $|u_{WKB}^{in}|$ reaches a local maximum. We took $R_{in}^* = \sqrt{2}\rho_{in}^*$ to be at the minimum of the hyperspherical potential $\varepsilon_2(R) - \frac{1}{2}\langle\varphi_2|(d^2\varphi_2/dR^2)\rangle$. We obtained the hyperspherical potential by using the finite element method to compute $\varepsilon_2'(R) = \varepsilon_2(R) - \frac{1}{2}(1/4/R^2)$ [49], and using the asymptotic form of the second derivative term, to order $1/R^4$, of Ref. [48]. Furthermore, we obtained $u^{in}(\rho_{in}^*)$ by evaluating at ρ_{in}^* the long-range form of the wave function which is written in terms of linear combination of Mathieu functions, and normalized according to Eq. (41). Classically, the ratio of the probability density per unit distance of finding the particles inside and outside the well is given by

$$K_{cl} = \left(\frac{k_2^2/2\mu}{k_2^2/2\mu + D} \right)^{1/2}, \quad (42)$$

where D is the depth of the well [36].

Figure 14(a) compares P , $|T|^2$, $\sigma_{12}(L=0)$, and $|T_{WKB}|^2$. For plotting purposes we normalized the variational results to unity at $k_2=0.077\,018$ a.u. There is reasonable agreement between P , $|T|^2$, and $\sigma_{12}(L=0)$ over a wide energy range, but $|T_{WKB}|^2$, even with the Langer correction, is quantitatively incorrect over most of the region. Figure 14(b) shows the threshold region in a more detail. The ratio P in the vicinity of the threshold scales approximately as the square root of the depth of the potential well. Interestingly, if one approximates for the depth of the well D by the magnitude of

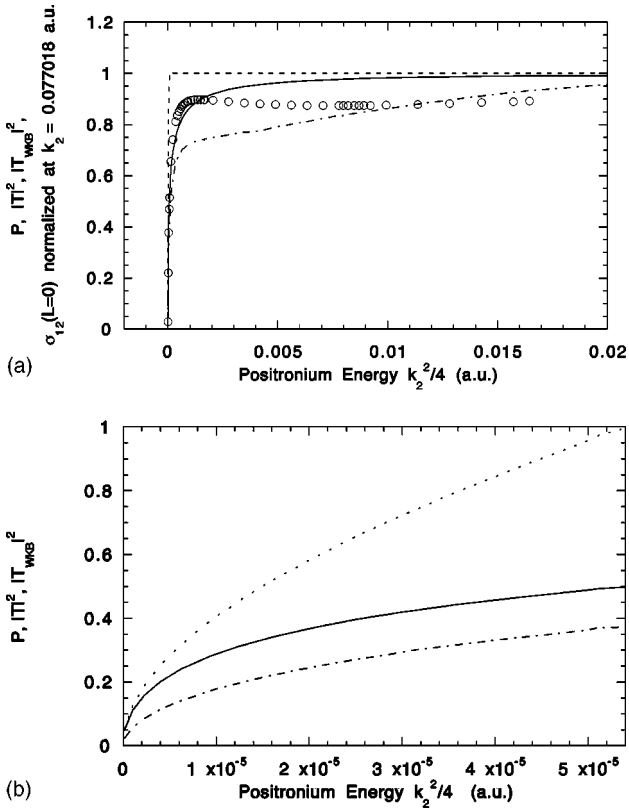


FIG. 14. (a) Comparison of the quantum suppression ratio P with the TOB factor $|T|^2$, with the WKB factor $|T_{WKB}|^2$, and with the variational results [14] for $\sigma_{12}(L=0)$ (normalized). For the figure we normalized the variational results $\sigma_{12}(L=0)$ at $k_2 = 0.077018$ a.u. ($k_2^2/4 = 1.482 \times 10^{-3}$ a.u.), which is at its peak value to the TOB factor $|T|^2$. The dash-dotted line is P , the solid line is $|T|^2$, the dashed line is $|T_{WKB}|^2$, and the open circles are the normalized variational results. (b) Comparison between the quantum suppression ratio P , the TOB factor $|T|^2$, and the WKB factor $|T_{WKB}|^2$, very close to the positronium formation threshold. See (a).

the polarization potential at ρ_{in}^* the ratio P is brought in quite good agreement with the factor $|T|^2$ for a positronium energy $k_2^2/2\mu$ to about 0.001 a.u.

We conclude that near-threshold S -wave positronium formation is an example of quantum suppression. The quantum suppression effects are satisfactorily modeled by ERT with the exact Mathieu functions, the top-of-barrier wave functions [45], or the quantum suppression factor P .

VI. CONCLUSIONS

Positron-hydrogen scattering is rich in low-energy features, including Ramsauer minima, virtual states, resonances, threshold phenomena, and quantum suppression. These features emerge in effective range theories that employ exact expressions for the Mathieu functions. The single-channel ERT of Fabrikant [34] and the multichannel ERT of Watanabe and Greene [33] use the exact expressions of the characteristic exponent τ and ratio m from the Mathieu functions. We used both ERT's to analyze partial wave cross sections for elastic positronium-proton scattering, and used the mul-

tichannel ERT to analyze partial wave cross sections for positronium formation in positron-hydrogen collisions. In addition to the ERT's, we used the top-of-barrier theory [29] and quantum suppression [36] to explore the threshold region. All the approaches take into account explicitly the significant polarization potential in the positronium-proton channel. The multichannel ERT, the top-of-barrier theory, and quantum suppression give the correct threshold behavior for S -wave positronium formation, and confirm that the range of validity of Wigner's threshold law is very narrow [15]. We find that the multichannel ERT fit even reproduces the small peak near threshold in the variational results, while the more approximate top-of-barrier and quantum suppression factors do not. For both $L=0$ and 1, the multichannel ERT fit to the variational calculations generally agree well with the *ab initio* calculations. For $L=2$, the multichannel ERT fits indicate that the variational calculations [14,42] are not reliable near threshold, whereas the E8PS calculations seem to be reliable.

The large S -wave scattering length in the positronium-proton channel is indicative of a virtual state. We located the pole in the S -matrix that corresponds to the S -wave virtual state of the positronium-proton system. The pole is displaced from the negative imaginary k axis because of the long-range polarization potential. The polarization affects the virtual state by shifting the pole slightly away from the negative imaginary axis. It also causes the phase shift to reach a maximum value of $\pi/8$ rather than $\approx \pi/2$, as expected for short-range potentials. It has long been recognized that Ramsauer minima require a strong polarization potential [50]. The virtual state in a strongly polarized system is an additional structure that more recently has been recognized [51,52].

For both $L=1$ and 2 we found a pole in the S matrix. Because the position E_r of the pole is negative but the width Γ is positive, the pole corresponds to a resonance with a negative energy position.

The behavior of the eigenphase corresponding to the positronium-proton channel is remarkably similar for all angular momenta. For $L=0$, there occurs a virtual state, and for $L=1$ and 2 a resonance at a negative energy position. There is a Ramsauer minimum in K_{22} for $L=0$ and 1, and in the diagonal element \tilde{K}_{22} for $L=0, 1$, and 2. Between the threshold and the minima, the eigenphase has a maximum value of $\pi/8(2L+1)$. We have not found a simple explanation for this maximum value. It appears to be an accidental feature of the positronium-proton channel not present in other systems.

In this paper we consider positron-hydrogen collisions specifically. However, many features of positronium formation and the elastic positronium-proton cross sections should be similar for all neutral targets, owing to the strong polarization potential in the positronium-ion channel. One notable difference for positron-alkali collisions is that positronium formation is possible at zero energy, and that at zero energy the S -wave cross section for positronium formation is infinite.

ACKNOWLEDGMENTS

We appreciate discussions with Dr. I. I. Fabrikant, Dr. T. T. Gien, Dr. J. Humberston, and Dr. P. Van Reeth. We thank

Dr. P. Van Reeth for providing us with their variational K matrices and cross sections. We also thank Dr. C. H. Greene and Dr. D. B. Khrebtukov for providing us with their FORTRAN codes. S.J.W. gratefully acknowledges support from the University of Tennessee, from the Institute for Theoretical Atomic and Molecular Physics at Harvard University and Smithsonian Astrophysical Observatory, from NSF under Grant No. PHY-9780016 and from a UNT faculty research grant. J.H.M gratefully acknowledges support from the NSF under Grant No. PHY-9222489. ORNL is managed by Lockheed Martin Energy Research Corp. under Contract No. DE-AC0596OR22464 with the U.S. DOE.

APPENDIX: VIRTUAL STATE AND RESONANCES

The association of large, low-energy, S -wave cross sections with loosely bound states or virtual states is a standard topic in elementary scattering theory [53–56]. The basic features of these states and resonances is well known for short-range potentials. In this appendix, we discuss what modifications occur to the position of a virtual state pole for $L=0$ and to a resonance pole for $L>0$, owing to the presence of the polarization potential.

We first recall some basic mathematical features of virtual states for short-range potentials. For single-channel S -wave scattering, the radial wave function has the asymptotic form

$$u \approx N[e^{-ikr} - S e^{ikr}], \quad (\text{A1})$$

where k can be any complex number. The function is analytically continued from positive real energy to negative energy by the replacement $k = i\kappa$, $\kappa > 0$, then

$$u \approx N[e^{\kappa r} - S e^{-\kappa r}] = NS[S^{-1} e^{\kappa r} - e^{-\kappa r}]. \quad (\text{A2})$$

For a bound state, $S^{-1} = 0$, i.e., S has a pole. For single-channel scattering, $S = e^{i2\delta_0}$, so that a pole corresponds to $\cot \delta_0 = i$. Using the first term in the ERT to write $\cot \delta_0$ as a function of k , and solving the equation $\cot \delta_0 = i$, gives a first estimate of the bound-state energy

$$\kappa \approx \frac{1}{a_0}. \quad (\text{A3})$$

The zero-energy cross section is given by

$$\sigma = 4\pi a_0^2 = \frac{4\pi}{\kappa^2} = \frac{2\pi}{|E_B|}, \quad (\text{A4})$$

which is large for a weakly bound state.

The zero-energy cross section is also large if the scattering length is large and negative, but in this case there is no bound state. Rather, the pole is at negative imaginary k , and the wave function increases exponentially at large distances. The corresponding state is unphysical, and is given the name virtual state. It can be considered as a new bound state about to be born [46]. Thus large, low-energy S -wave cross sec-

tions are usually associated with loosely bound states or virtual states. For short-range potentials the low-energy phase shift is often approximately given by $\tan \delta_0 \approx a_0 k$, and if a_0 is large the phase shift increases rapidly with increasing energy, but does not exceed $\pi/2$, i.e., $\tan \delta_0$ does not become infinite.

Large cross sections are also associated with resonances corresponding to poles at complex energies $E_r - i\Gamma/2$ with the position E_r and the width Γ both positive. In the k plane these occur at $k_r - ik_i$, with k_r and k_i both positive. Symmetry requirements show that there are mirror poles at the same value of k_i and negative k_r .

To see how these properties are modified by the polarization potential, consider the estimate of the pole position using the first two terms of the MERT. One finds

$$k_2 = k_{2p} = k_r + ik_i = \frac{\frac{1}{a_0} \frac{\pi\mu\alpha}{3a_0^2}}{1 + \left(\frac{\pi\mu\alpha}{3a_0^2}\right)^2} + \frac{\frac{i}{a_0}}{1 + \left(\frac{\pi\mu\alpha}{3a_0^2}\right)^2}. \quad (\text{A5})$$

Because the scattering length is negative, both k_r and k_i are negative, i.e., the pole is shifted slightly off the negative imaginary axis. Only in the limiting case $\alpha \rightarrow 0$ is the pole on negative imaginary axis at $k_i = i/a_0$.

In the energy plane the pole occurs at

$$E_{2p} = \frac{k_r^2 - k_i^2}{2\mu} + \frac{2ik_r k_i}{2\mu}. \quad (\text{A6})$$

For $L=0$, the imaginary part of E_{2p} is positive, i.e., the width Γ is negative. The pole does not correspond to a resonance but to a virtual state shifted off the imaginary axis. The effect of the polarization potential is to shift the position of the pole in the k plane toward the left from the position it would have for a short-range interaction. If one uses the ERT of Fabrikant [34] with constant M , rather than the MERT, the position of the pole moves to $E_{2p} = -0.00034 + 0.00002i$, but E_r and Γ are still negative.

For short-range interactions, $k \cot \delta_0$ is an analytic function of energy, however, this is not the case for inverse power-law potentials. The nonanalyticity can be traced to the nonanalyticity of the ratio m [$m = (fk)^\tau$], since τ is not an integer. With the MERT we located a single pole to the left of the negative imaginary k axis. We could not locate a mirror pole, i.e., a pole to the right of the negative imaginary k axis; however, it could lie on a different sheet of the Riemann surface.

There are examples of virtual states for long-range interactions in which the position of the pole is displaced off the negative imaginary k -axis. For instance, Herzenberg and Saha [46] obtained a virtual electron state in a weakly polar molecule. The state is predominately S -wave character. The tail of the potential is a dipole potential. The pole which corresponds to a virtual state is off the negative imaginary k

axis, and, to the left of it, on the physical sheet of the Riemann surface. (The first sheet is defined by a cut along the negative real axis.) There is a corresponding pole that is symmetric about the negative imaginary k axis, but this pole occurs on a different Riemann sheet. Other examples of poles off the negative imaginary k axis that do not correspond to resonances have been given by Fabrikant [51,57], and Hill *et al.* [58].

The Mathieu functions with angular momentum $L > 0$ are not qualitatively different from those with $L = 0$. For $L = 1$ and 2 we also located poles in the single-channel S matrix.

Using the single-channel ERT of Fabrikant with constant M we found poles at $k_{2p} = 0.095 - 0.168i$ for $L = 1$ and at $k_2 = 0.2569 - 0.3129i$ for $L = 2$. In both cases the poles occur at negative energies, but the width $\Gamma = -4k_r k_i$ is positive. Thus these poles correspond to resonances at a negative energy position. As for $L = 0$, the effect of the polarization potential is to shift the pole in the k plane to the left. For $L = 1$ and 2, the magnitude of the real part of the pole in the k plane $|k_r|$ has been reduced to be less than the magnitude of the imaginary part $|k_i|$. This has the consequence that in the energy plane the position E_r of the pole is negative.

-
- [1] W. Sperber, D. Becker, K.G. Lynn, W. Raith, A. Schwab, G. Sinapius, G. Spicher, and M. Weber, *Phys. Rev. Lett.* **68**, 3690 (1992).
- [2] M. Weber, A. Holmann, W. Raith, W. Sperber, F. Jacobsen, and K.G. Lynn, *Hyperfine Interact.* **89**, 221 (1994).
- [3] S. Zhou, H. Li, W.E. Kauppila, C.K. Kwan, and T.S. Stein, *Phys. Rev. A* **55**, 361 (1996).
- [4] V. Kara, K. Paludan, J. Moxom, and G. Laricchia, in *Scientific Program, and Abstracts of Contributed Papers of the XX International Conference on the Physics of Electronic, and Atomic Collisions, Vienna, Austria, 23-29 July, 1997*, edited by F. Aumayr, G. Betz, and H.P. Winter, 1997, Vol. I, p. TH080 (unpublished).
- [5] H.S.W. Massey, *Can. J. Phys.* **60**, 461 (1982).
- [6] M. Leventhal, and B.L. Brown, in *Proceedings of the Third International Workshop on Positron (Electron)-Gas Scattering*, edited by W.E. Kauppila, T.S. Stein, and J. Wadehra (World Scientific, Singapore, 1986), p. 140.
- [7] E. Stokstad, *Science* **276**, 897 (1997).
- [8] J.W. Humberston, M. Charlton, F.M. Jacobsen, and B.I. Deutsch, *J. Phys. B* **20**, L25 (1987).
- [9] J.W. Humberston, *Can. J. Phys.* **60**, 591 (1982).
- [10] J.W. Humberston, *J. Phys. B* **17**, 2353 (1984).
- [11] C.J. Brown and J.W. Humberston, *J. Phys. B* **17**, L423 (1984).
- [12] C.J. Brown and J.W. Humberston, *J. Phys. B* **18**, L401 (1985).
- [13] J.W. Humberston, *Adv. At. Mol. Phys.* **22**, 1 (1986).
- [14] J.W. Humberston, P. Van Reeth, M.S.T. Watts, and W.E. Meyerhof, *J. Phys. B* **30**, 2477 (1997); P. Van Reeth, and J.W. Humberston (private communication).
- [15] E.P. Wigner, *Phys. Rev.* **73**, 1002 (1948).
- [16] M.T. McAlinden, A.A. Kernoghan, and H.R.J. Walters, *Hyperfine Interact.* **89**, 161 (1994).
- [17] A.A. Kernoghan, M.T. McAlinden, and H.R.J. Walters, *J. Phys. B* **28**, 1079 (1995).
- [18] A.A. Kernoghan, D.J.R. Robinson, M.T. McAlinden, and H.R.J. Walters, *J. Phys. B* **29**, 2089 (1996).
- [19] J. Mitroy, L. Berge, and A. Stelbovics, *Phys. Rev. Lett.* **73**, 2966 (1994).
- [20] J. Mitroy, *Aust. J. Phys.* **48**, 646 (1995).
- [21] J. Mitroy, *J. Phys. B* **29**, L263 (1996).
- [22] T.T. Gien, *Phys. Rev. A* **56**, 1332 (1997).
- [23] B.J. Archer, G.A. Parker, and R.T. Pack, *Phys. Rev. A* **41**, 1303 (1990).
- [24] A. Igarashi and N. Toshima, *Phys. Rev. A* **50**, 232 (1994).
- [25] Y. Zhou and C.D. Lin, *J. Phys. B* **27**, 5065 (1994).
- [26] Y. Zhou, and C.D. Lin, *J. Phys. B* **28**, 4907 (1995).
- [27] Y. Zhou and C.D. Lin, *Can. J. Phys.* **74**, 353 (1996).
- [28] Chi-Yu Hu, *Phys. Rev. A* **59**, 4813 (1999).
- [29] S.J. Ward, J.H. Macek, and S.Yu. Ovchinnikov, *Phys. Rev. A* **59**, 4418 (1999).
- [30] S. Zhou, S.P. Parikh, W.E. Kauppila, C.K. Kwan, D. Lin, A. Surdutovich, and T.S. Stein, *Phys. Rev. Lett.* **73**, 236 (1994).
- [31] W.E. Meyerhof, and G. Laricchia, *J. Phys. B* **30**, 2221 (1997).
- [32] A.M. Lane and R.G. Thomas, *Rev. Mod. Phys.* **30**, 257 (1958).
- [33] S. Watanabe and C.H. Greene, *Phys. Rev. A* **22**, 158 (1980).
- [34] I.I. Fabrikant, *Opt. Spektrosk* **53**, 223 (1982) [*Opt. Spectrosc.* **53**, 131 (1982)].
- [35] P. Van Reeth and J.W. Humberston, *J. Phys. B* **31**, L621 (1998).
- [36] R. Côté, E.R. Heller, and A. Dalgarno, *Phys. Rev. A* **53**, 234 (1996).
- [37] T.F. O'Malley, L. Spruch, and L. Rosenberg, *J. Math. Phys.* **2**, 491 (1961).
- [38] E. Vogt and G.H. Wannier, *Phys. Rev.* **95**, 1190 (1954).
- [39] M.J. Cavagnero, *Phys. Rev. A* **50**, 2841 (1994).
- [40] D.B. Khrebtukov, *J. Phys. A* **26**, 6357 (1993); and Fortran Code, 1998 (unpublished).
- [41] S. Watanabe and C. H. Greene, Fortran Code; C.H. Greene (private communication).
- [42] P. Van Reeth (private communication).
- [43] T.T. Gien, *J. Phys. B* **30**, L23 (1997).
- [44] R. Damburg and E. Karule, *Proc. Phys. Soc. London* **90**, 637 (1967).
- [45] J.H. Macek and S.Yu. Ovchinnikov, *Phys. Rev. A* **50**, 468 (1994).
- [46] A. Herzenberg and B.C. Saha, *J. Phys. B* **16**, 591 (1983).
- [47] J.H. Macek and S.Yu. Ovchinnikov, *Phys. Rev. A* **54**, 544 (1996).
- [48] M. Cavagnero, Z. Zhen, and J. Macek, *Phys. Rev. A* **41**, 1225 (1990).
- [49] J. Shertzer and S.J. Ward (private communication).
- [50] N.F. Mott and H.S.W. Massey, *The Theory of Atomic Collisions*, 3rd ed. (Oxford University Press, Oxford, 1965).
- [51] I.I. Fabrikant, *Comments At. Mol. Phys.* **32**, 267 (1996).
- [52] C. Bahrim and U. Thumm, *Phys. Rev. A* **61**, 22722 (2000).
- [53] T. Wu and T. Ohmura *Quantum Theory of Scattering* (Prentice-Hall, Englewood Cliffs, NJ, 1962).

- [54] R.G. Newton *Scattering Theory of Waves and Particles* (McGraw-Hill, New York, 1966).
- [55] C.J. Joachain, *Quantum Collision Theory*, 3rd ed. (North-Holland, Amsterdam, 1983).
- [56] P.G. Burke and C.J. Joachain, *Theory of Electron-Atom Collisions, Part 1: Potential Scattering* (Plenum Press, New York, 1995).
- [57] I.I. Fabrikant, *J. Phys. B* **18**, 1873 (1985).
- [58] S.B. Hill, M.T. Frey, F.B. Dunning, and I.I. Fabrikant, *Phys. Rev. A* **53**, 3348 (1996).